Ti-STT: A new zeotype shape selective oxidation catalyst

Ti-STT: A new zeotype shape selective oxidation catalyst

Einar André Eilertsen, Filippo Giordanino, Carlo Lamberti, Silvia Bordiga, Alessandro Damin, Francesca Bonino, Unni Olsbye and Karl Petter Lillerud

Chem. Commun., 2011, **47**, 11867–11869

DOI: 10.1039/c1cc15175d

Ti-STT: A new zeotype shape selective oxidation catalyst

Einar André Eilertsen,[a] Filippo Giordanino[b], Carlo Lamberti [*b], Silvia Bordiga[b], Alessandro Damin[b], Francesca Bonino[b], Unni Olsbye[a] and Karl Petter Lillerud[*a]

A new zeotype titanium silicate oxidation catalyst with the STT topology has been synthesized from direct synthesis. Ti-STT has a microporous structure with small pore openings, allowing shape selective oxidation catalysis. The isomorphous substitution of Si by Ti in the framework has been confirmed by Raman, FT-IR, UV-VIS and XANES spectroscopies.

Titanium silicalite-1 (TS-1), with the MFI topology, was the first titanium silicate with a zeolite topology to be reported.[1] TS-1 shows excellent properties as a shape selective oxidation catalyst with high activity at mild conditions, and is now of great industrial importance.[2] The relevance of this catalyst on the industrial ground makes the research on the catalyst improvement still active nowadays, i.e. almost thirty years after its first patent. Improvements reflect: (i) the growth of TS-1 crystals with controllable *b*-oriented length (sheet-like morphology, or chain-like morphology);[3,4] (ii) the synthesis of hierarchical mesoporous TS-1;[5-7] (iii) synthesis of Au/TS-1 catalysts for in situ production of hydrogen peroxide;[8] (iv) co-insertion of other heteroatom in the MFI framework;[9] (v) synthesis of amorphous[10] or crystalline porous titanosilicates with different topologies, such as TS-2,[11] Ti-β,[12] Ti-UTD-1,[13] Ti-ZSM-48[14] Ti-MOR,[15] Ti-FER,[16] Ti-ITQ-6,[17] delaminated Ti-ITQ-2,[18] Ti-MCM-22,[19] Ti-MCM-56,[19] Ti-MWW,[20] Ti-JLU- 20,[21] Ti-MCM-68[22] and more recently Ti-CHA;[23]

STT is a zeolite topology with a 2-dimensional pore system composed of a 7- and 9-ring channel system.[24,25] While the previous titanium silicates have 10-ring pores or larger, this material has smaller pores, opening new possibilities in shape selective catalysis. SSZ-23 was the first STT material to be synthesized by Zones et al. using N,N,N-trimethyl-adamantammonium hydroxide (TMAdaOH) as structure directing agent.[26]

To produce the Ti-STT with Si/Ti = 106, the following procedure was employed: 4 g Ethanol, 6.5 g tetraethyl orthosilicate, 0.15 g titanium (IV) ethoxide and 0.15 g H_2O_2 (30 wt%) were mixed and added dropwise to 15 g 1M TMAdaOH. The mixture was hydrolyzed over night and heated to evaporate ethanol and H_2O. Then 0,7 g HF (40%) was added, giving a final H_2O/SiO_2 ratio of 10, and the resulting dry gel was transferred to a 15 mL teflon lined stainless steel autoclave and heated for 10 days in a tumbling oven at 35 rpm at 155 ^oC. A yield of 70% was obtained.

Powder XRD of the materials in Fig. 1 is characteristic of the STT topology with high crystallinity and without TiO_2-anatase, TiO_2-rutile or other impurities. SEM (Fig S1) shows platelets with size of 20 x 15 x 1 µm, while elemental analysis in Table 1 shows that 47 % of the Ti in the synthesis gel was finally incorporated into the material.

The isomorphous substitution of Si by Ti in the STT framework has been confirmed by Raman-, FTIR, DRUV-VIS- and XANES spectroscopies. It is known that Ti substitution in TS-1 perturbs the stretching modes of adjacent [SiO_4] units resulting in two components at 960 cm^{-1} and 1125 cm^{-1}, the latter visible by Raman only.[12,27-32] In hydrated Ti-STT the asymmetric modes occurs at 967 and 970 cm^{-1} in the FTIR and Raman (Figs S3 and 2a) spectra, respectively (once dehydrated the band red-shifts at 953 cm^{-1}, red curve in the inset of Fig. 2a). The totally symmetric stretching of the [TiO_4] units is observed at 1118 cm^{-1} (Fig 2b). These modes are absent in the case of the pure SiO_2-STT material (black curves in Fig 2a). Raman spectroscopy also shows no traces of TiO_2-anatase as there is no peak at 637 cm^{-1}. As seen from Fig 2b, the 1118 cm^{-1} peak is enhanced in intensity with respect to the 960 cm^{-1} peak as the wavelength approaches the charge-transfer (CT) transition (325 nm pre-resonance and 244 nm resonance conditions), similar to what has been observed for TS-1.[28-30]

Table 1 Reaction conditions: Batch reactor. Solvent methanol = 13 g. Catalyst = 0.2 g, H_2O_2 = 2.67 g (30 wt %). T = 333K. Time = 6 h.

Material	Si/Ti		% Ti incorporated	Ethane oxide selectivity (%)	H_2O_2 conversion (%)
	In gel	In material			
Ti-STT	50	106	47	49	48
TS-1	50	56	89	62	93

DRS UV-VIS spectroscopy of the calcined sample activated in vacuum at 500 ^oC (red curve in Fig 3a) shows a band at 48000 cm^{-1} which can be assigned to a ligand to metal charge transfer (LMCT) for isolated Ti-tetrahedra.[28-31] No tail, due to extra framework TiO_2-anatase, can be observed. The interaction with H_2O causes a red shift of the edge in the DRUV-VIS spectrum. This is an expected consequence of the increase in coordination sphere around Ti(IV) centers.[31,32]

The XANES spectra of the Ti-STT material dehydrated at 500 ^oC directly proves that Ti species exhibit a local T_d symmetry, as testified by the intense and sharp pre edge peak due to the 1s → 3p electronic transition (blue spectrum in Fig 3b).[27,31] Ti(IV) species ($3p^6 3d^0$) exhibit a significant density of unoccupied 3*p* states only when a strong 3*p*/3*d* hybridization is present, i.e. in case of T_d symmetry that exhibits no inversion center. Coordination of water distorts the T_d symmetry towards an O_h-like one where the 3*p*/3*d* hybridization is much less efficient and the intensity of the pre edge peak drops (red spectrum in Fig. 3b).

The IR, DRUV-VIS and XANES dehydration experiments reported in Figs S4 and 3 shows that Ti(IV) species hosted in the framework are able to modify their local geometry upon interaction with adsorbates (H_2O) and are so potential catalytic centres.

The catalytic activity and selectivity of the material was tested using the epoxidation of ethene with H_2O_2 as a model reaction and compared to the performance of TS-1. As seen from Table 1, the conversion of H_2O_2 is 49 % and the selectivity towards ethylene oxide is 48 %. The reactant shape selective properties of the new material are proven by the epoxidation of hexene and the hydroxylation of phenol. While many other titanium zeotypes exhibit high activity,[20,33] the Ti-STT is essentially inactive due to the smaller pore openings. The kinetic diameter of hex-1-ene is in principle small enough to allow the molecule to enter the 9-ring pores of STT (5,3x3,7 Å), but the long aliphatic tail will make diffusion extremely slow. Phenol, however, is excluded from the pore system due to the higher kinetic diameter of the molecule (4,8 Å).[34] The catalytic activity supports the conclusion from spectroscopic studies that Ti is incorporated in the tetrahedral framework.

On a spectroscopic ground, the reactivity of Ti-STT toward H_2O_2/H_2O solution is testified by the DRS-UV-Vis, XANES and Raman spectra reported in Fig. 4. The formation of a side-on peroxo complex on Ti sites is confirmed by the three techniques. The yellow colour of the Ti-STT/H_2O_2/H_2O system is due CT from the peroxo ligand to the Ti around 29000 cm^{-1} (Fig. 4a). The same CT occurs at 26000 cm^{-1} in the TS-1/H_2O_2/H_2O system[27,30,35], and at 31000 cm^{-1} in the $Na_3TiF_5O_2$ model compound (vine curve in Fig. 4a). The XANES spectrum of the Ti-STT/H_2O_2/H_2O system is characterized by the doublet at 4987 and 4999 eV on the edge (Fig. 4b).[30.36] The vibrational feature of the side-on Ti-peroxo complex re easily caught by Raman spectroscopy using a 442 nm laser because it allows resonant conditions with the corresponding CT.[30,35] As a consequence of the resonant enhancement, the Raman spectrum of the Ti-STT/H_2O_2/H_2O system (Fig. 4c) is dominated by two bands at 876 and 626 cm-1 due to the O-O stretching and to the and to the symmetric breathing mode of the $Ti(O)_2$ cycle, respectively.[35]

In summary we have synthesized a new microporous zeotype titanium silicate with the STT topology. This is a small pore zeotype titanium silicate and it shows catalytic activity in epoxidation of ethene.

We are indebted with the whole staff of BM26B[37] at the ESRF (and in particularly with S. Nikitenko) and to D. Gianolio and E. Borfecchia for the XANES data collection. E.A.E. gratefully acknowledge financial support from the Norwegian research council (KOSKII) and Sachem Inc for supplying us with TMAdaOH (ZeoGen 2825).

Notes and references

[a] SMN/INGAP/Departement of Chemistry. University of Oslo Sem Selands vei 26, 0315 Oslo, Norway E/mail: kpl@kjemi.uio.no

[b] Department of Inorganic, Physical and Materials Chemistry NIS Centre of Excellence, and INSTM reference center, University of Turin, Via P. Giuria 7, I-10125 Torino, 4 Italy. Tel: +39 011 6707841 E-mail: carlo.lamberti@unito.it

† Electronic Supplementary Information (ESI) available: [SEM, FT-IR, UV-VIS, XRD and experimental details]. See DOI: 10.1039/b000000x/

1 M. Taramasso, G. Perego and B. Notari, **1983**, US Patent No. 4410501.
2 B. Notari, *Adv. Catal.*, 1996, **41**, 253.
3 X. D. Wang, B. Q. Zhang, X. F. Liu and J. Y. S. Lin, *Adv. Mater.*, 2006, **18**, 3261.
4 M. R. Kishan, J. Tian, P. K. Thallapally, C. A. Fernandez, S. J. Dalgarno, J. E. Warren, B. P. McGrail and J. L. Atwood, *Chem. Commun.*, 2010, **46**, 538.
5 I. Schmidt, A. Krogh, K. Wienberg, A. Carlsson, M. Brorson and C. J. H. Jacobsen, *Chem. Commun.*, 2000, 2157.
6 D. Serrano, R. Sanz, P. Pizarro and I. Moreno, *Chem. Commun.*, 2009, 1407.
7 J. A. Zhou, Z. L. Hua, X. Z. Cui, Z. Q. Ye, F. M. Cui and J. L. Shi, *Chem. Commun.*, 2010, **46**, 4994.
8 J. J. Bravo-Suarez, K. K. Bando, T. Akita, T. Fujitani, T. J. Fuhrer and S. T. Oyama, *Chem. Commun.*, 2008, 3272.
9 R. Klaewkla, S. Kulprathipanja, P. Rangsunvigit, T. Rirksomboon and L. Nemeth, *Chem. Commun.*, 2003, 1500.
10 J. M. Thomas and G. Sankar, *Accounts Chem. Res.*, 2001, **34**, 571.
11 A. Thangaraj, R. Kumar and P. Ratnasamy, *J. Catal.*, 1991, **131**, 294.
12 (*a*) T. Blasco, M. Camblor, A. Corma and J. Pérez-Parriente, *J. Am. Chem. Soc.*, 1993, **115**, 11806. (*b*) M. A. Camblor, A. Corma and J. Perezpariente, *Chem. Commun.*, 1993, 557.
13 R. J. Saxton, *Top. Catal.*, 1999, **9**, 43.
14 J. LeBars, J. Dakka and R. A. Sheldon, *Appl. Catal. A-Gen.*, 1996, **136**, 69.
15 P. Wu, T. Komatsu and T. Yashima, *J. Phys. Chem. B*, 1998, **102**, 9297.
16 A. Corma, U. Diaz, M. E. Domine and V. Fornes, *Chem. Commun.*, 2000, 137.
17 A. Corma, U. Diaz, M. E. Domine and V. Fornes, *J. Am. Chem. Soc.*, 2000, **122**, 2804.
18 A. Corma, U. Diaz, V. Fornes, J. L. Jorda, M. Domine and F. Rey, *Chem. Commun.*, 1999, 779.
19 A. Corma, U. Diaz, V. Fornes, J. M. Guil, J. Martinez-Triguero and E. J. Creyghton, *J. Catal.*, 2000, **191**, 218.
20 P. Wu and T. Tatsumi, *Chem. Commun.*, 2001, 897.
21 X. Y. Yang, Y. Han, K. F. Lin, G. Tian, Y. F. Feng, X. J. Meng, Y. Di, Y. C. Du, Y. L. Zhang and F. S. Xiao, *Chem. Commun.*, 2004, 2612.
22 Y. Kubota, Y. Koyama, T. Yamada, S. Inagaki and T. Tatsumi, *Chem. Commun.*, 2008, 6224.
23 E. A. Eilertsen, S. Bordiga, C. Lamberti, A. Damin, F. Bonino, B. Arstad, S. Svelle, U. Olsbye and K. P. Lillerud, *ChemCatChem*, 2011, in press.
24 M. A. Camblor, M. J. Diaz-Cabanas, J. Perez-Pariente, S. J. Teat, W. Clegg, I. J. Shannon, P. Lightfoot, P. A. Wright and R. E. Morris, *Angew. Chem.-Int. Edit.*, 1998, **37**, 2122.
25 M. A. Camblor, M. J. Diaz-Cabanas, P. A. Cox, I. J. Shannon, P. A. Wright and R. E. Morris, *Chem. Mat.*, 1999, **11**, 2878.
26 S. I. Zones, **1989**, US. Pat. 4,859,442.
27 S. Bordiga, S. Coluccia, C. Lamberti, L. Marchese, A. Zecchina, F. Boscherini, F. Buffa, F. Genoni, G. Leofanti, G. Petrini and G. Vlaic, *J. Phys. Chem.*, 1994, **98**, 4125.
28 G. Ricchiardi, A. Damin, S. Bordiga, C. Lamberti, G. Spanò, F. Rivetti and A. Zecchina, *J. Am. Chem. Soc.*, 2001, **123**, 11409.
29 C. Li, G. Xiong, Q. Xin, J. Liu, P. Ying, Z. Feng, J. Li, W. Yang, Y. Wang, G. Wang, X. Liu, M. Lin, X. Wang and E. Min, *Angew. Chem. Int. Ed.*, 1999, **38**, 2220.
30 S. Bordiga, A. Damin, F. Bonino, G. Ricchiardi, A. Zecchina, R. Tagliapietra and C. Lamberti, *Phys. Chem. Chem. Phys.*, 2003, **5**, 4390.
31 S. Bordiga, F. Bonino, A. Damin and C. Lamberti, *Phys. Chem. Chem. Phys.*, 2007, **9**, 4854.
32 S. Bordiga, A. Damin, F. Bonino, A. Zecchina, G. Spanò, F. Rivetti, V. Bolis and C. Lamberti, *J. Phys. Chem. B*, 2002, **106**, 9892.
33 (a) A. Corma, U. Diaz, M. E. Domine and V. Fornes, *Angew. Chem.-Int. Edit.*, 2000, **39**, 1499; (b) M.G. Clerici, in: *Metal Oxide Catalysis* (S. D. Jackson and J. S. J. Hargreaves, Eds.), Wiley-VCH, Weinheim, 2008. Vol. 2, Chapter 18, p.705.
34 T. Atoguchi, T. Kanougi, T. Yamamoto, S. Yao, *J. Mol. Catal. A: Chem.*, 2004, **220**, 183.
35 S. Bordiga, A. Damin, F. Bonino, G. Ricchiardi, C. Lamberti and A. Zecchina, *Angew. Chem. Int. Ed.*, 2002, **41**, 4734.
36 (*a*) F. Bonino, A. Damin, G. Ricchiardi, M. Ricci, G. Spanò, R. D'Aloisio, A. Zecchina, C. Lamberti, C. Prestipino and S. Bordiga, *J. Phys. Chem. B*, 2004, **108**, 3573; (*b*) C. Prestipino, F. Bonino, A. Usseglio, A. Damin, A. Tasso, M. G. Clerici, S. Bordiga, F. D'Acapito, A. Zecchina and C. Lamberti, *ChemPhysChem.*, 2004, **5**, 1799.

37 G. Silversmit, B. Vekemans, S. Nikitenko, W. Bras, V. Czhech, G. Zaray, I. Szaloki and L. Vincze, *J. Synchrot. Radiat.*, 2009, **16**, 237.

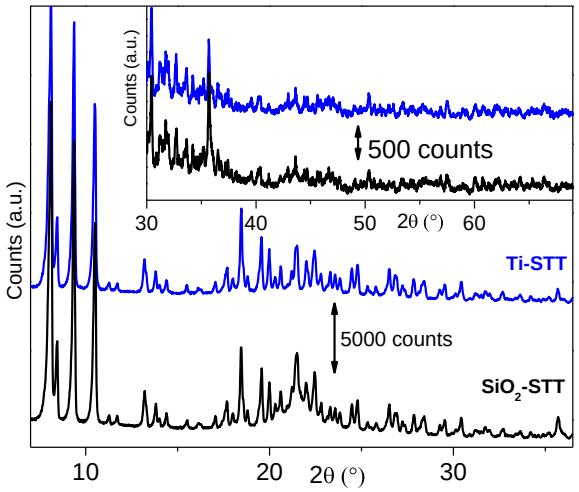

Fig. 1 Powder XRD of the calcined Ti-STT (blue) and SiO_2-STT (black). Main part: low 2θ region ; inset: high 2θ region. λ = 1.540 Å.

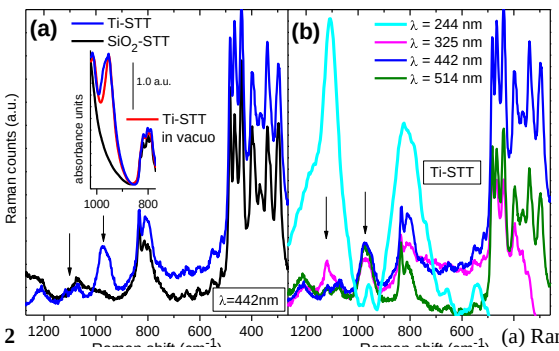

Fig. 2 (a) Raman spectroscopy of Ti-STT (blue) and SiO_2-STT (black) λ = 442 nm. The inset reports, in the narrow IR transparent window the 950 cm^{-1} band of Ti-STT and how it red shifts upon water desorption (red): a. u. = absorbance units. (b) Raman spectra of Ti-STT with 244 (cyan) 325 nm (magenta), 442 nm (blue) and 514 nm (green) laser. In both parts the 1118 cm^{-1} and 970 cm^{-1} peaks are marked with arrow. Raman spectre were collected on the hydrated forms. When using lasers with shorter excitation λ (325 and 255 nm), the low-energy cut-off needed to discard the elastic scattering occurs at lower wavenumbers.

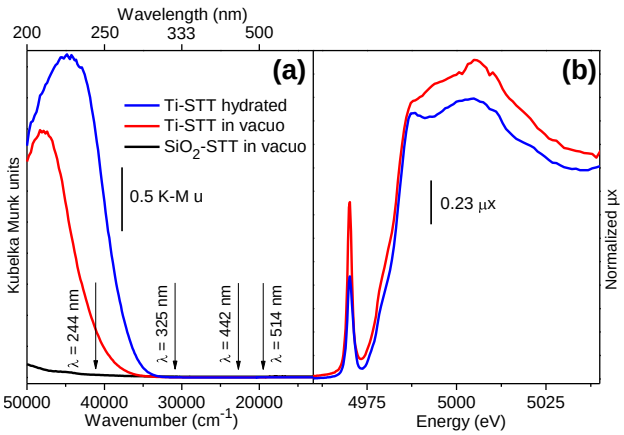

Fig. 3 DRS-UV-VIS and Ti K-edge XANES spectra of dehydrated (red) and hydrated (blue) Ti-STT, parts (a) and (b), respectively. In (a) also the spectrum of SiO_2-STT has been reported (black). Arrows in (a) indicate the excitation energies of lasers used to collect the Raman spectra in Fig. 2b.

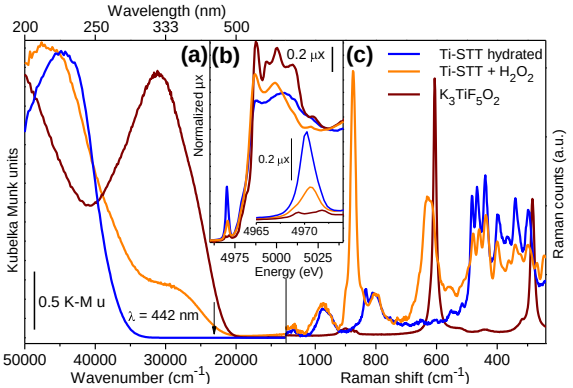

Fig. 4. DRS-UV-VIS, XANES and Raman (λ = 442 nm) spectra of Ti-STT contacted with H_2O_2/H_2O solution (orange curves), parts (a), (b) and (c), respectively. For comparison also the spectra of hydrated Ti-STT and of $Na_3TiF_5O_2$ model compound (see cartoon in part a) have been reported. The inset in part (b) reports a zoom on the pre-edge peak.

----------Figure and text for the Table of Contents --------

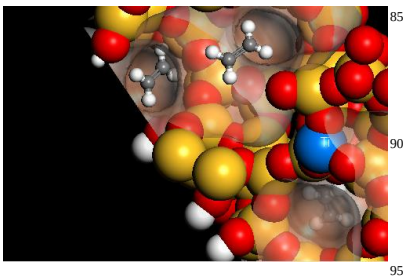

A new titanosilicate molecular sieve has been syntesixed with STT topology. Isomorphous insertion of Ti in the framework has been documented by UV-Vis, IR, Raman and XANES spectroscopies. Catalitic activity has been documented for ethylene epoxidation.